

Tumor subclones, where are you?

Xianbin Su^{1#,*}, Shihao Bai^{1#}, Gangcai Xie^{2#}, Yi Shi^{3#}, Linan Zhao¹, Guoliang Yang⁴,
Futong Tian⁵, Kun-Yan He¹, Lan Wang¹, Xiaolin Li¹, Qi Long^{6*}, Ze-Guang Han^{1*}

¹ Key Laboratory of Systems Biomedicine (Ministry of Education), Shanghai Center for Systems Biomedicine, Shanghai Jiao Tong University, Shanghai, China.

² Institute of Reproductive Medicine, Medical School of Nantong University, Nantong, China.

³ Bio-X Institutes, Key Laboratory for the Genetics of Developmental and Neuropsychiatric Disorders, Shanghai Jiao Tong University, Shanghai, China.

⁴ Department of Urology, Renji Hospital, Shanghai Jiao Tong University School of Medicine, Shanghai, China.

⁵ Department of Design, Politecnico di Milano, Milan, Italy.

⁶ Joint School of Life Sciences, Guangzhou Medical University & Guangzhou Institutes of Biomedicine and Health-Chinese Academy of Sciences, Guangzhou, China.

#Equal contribution.

*Correspondence:

Xianbin Su, Key Laboratory of Systems Biomedicine (Ministry of Education), Shanghai Center of Systems Biomedicine, Shanghai Jiao Tong University, 800 Dongchuan Road, Shanghai 200240, China. Tel: +86-21-3420-4150; Fax: +86-21-3420-6059; Email: xbsu@sjtu.edu.cn

Qi Long, Joint School of Life Sciences, Guangzhou Medical University & Guangzhou Institutes of Biomedicine and Health-Chinese Academy of Sciences, 1st Xinzao Road, Guangzhou 511436, China. Tel & Fax: +86-20-3201-5340; Email: long_qi@gibh.ac.cn

Ze-Guang Han, Key Laboratory of Systems Biomedicine (Ministry of Education), Shanghai Center of Systems Biomedicine, Shanghai Jiao Tong University, 800 Dongchuan Road, Shanghai 200240, China. Tel: +86-21-3420 7304; Fax: +86-21-3420-6059; Email: hanzg@sjtu.edu.cn

Running title: tumor clonal structure requires single-cell dissection

34 **Abstract**

35 **Introduction:** Tumor clonal structure is closely related to future progression,
36 which has been mainly investigated via mutation abundance clustering in bulk sample.
37 With limited studies at single-cell resolution, a systematic comparison of the two
38 approaches is still lacking.

39 **Methods:** Here, using bulk and single-cell mutational data from liver and
40 colorectal cancers, we would like to check the possibility of obtaining accurate tumor
41 clonal structures from bulk-level analysis. We checked whether co-mutations
42 determined by single-cell analysis had corresponding bulk variant allele frequency
43 (VAF) peaks. We examined VAF ranges for different groups of co-mutations, and also
44 the possibility of discriminating them.

45 **Results:** While bulk analysis suggested absence of subclonal peaks and possibly
46 neutral evolution in some cases, single-cell analysis identified co-existing subclones.
47 The overlaps of bulk VAF ranges for co-mutations from different subclones made it
48 difficult to separate them, even with other parameter introduced. The difference
49 between mutation cluster and tumor subclone is accountable for the challenge in bulk
50 clonal deconvolution, especially in case of branched evolution as shown in colorectal
51 cancer.

52 **Conclusion:** Complex subclonal structures and dynamic evolution are hidden
53 under the seemingly clonal neutral pattern at bulk level, suggesting single-cell
54 analysis will be needed to avoid under-estimation of tumor heterogeneity.

55

56 **Research Highlights**

- 57 ● Bulk-level mutation abundance clusters are not equal to tumor subclones.
- 58 ● Different groups of co-mutations could not be discriminated at bulk-level.
- 59 ● Single-cell mutational analysis can identify rather than infer tumor subclones.
- 60 ● Co-existing tumor subclones may have clonal neutral appearance at bulk-level.

61

62 **Lay summary**

63 Systematic comparison of tumor clonal structure differences between bulk and
64 single-cell mutational analysis is lacking. Here we performed such as study and found
65 that complex subclonal structures and dynamic evolution are hidden under clonal
66 neutral appearance at bulk level in liver and colorectal cancers, suggesting single-cell
67 analysis will be needed to avoid under-estimation of tumor heterogeneity.

68

69 **Keywords**

70 Genetic heterogeneity; clonal structure; tumor evolution; variant allele frequency;
71 single-cell analysis

72

73 **Introduction**

74 Tumor is generally believed to be originated from mutations in a single cell, but
75 when diagnosed the tumor mass usually contains large populations of progenies with
76 different mutations and form subclones (Cairns, 1975; Nowell, 1976). The clonal
77 structure and evolution within a tumor is closely related to its future progression such
78 as treatment response and metastasis (Greaves and Maley, 2012; Marusyk et al., 2020;
79 Yates and Campbell, 2012; Zahir et al., 2020). There are currently accumulative
80 genomic data from bulk tumor tissues, providing insights on intra-tumor genetic
81 heterogeneity (Dentro et al., 2021; Gerstung et al., 2020; Jamal-Hanjani et al., 2017;
82 Turajlic et al., 2018). Many tools have also been developed to investigate tumor
83 clonal structures based on the distribution of variant allele frequency (VAF) values
84 from bulk samples, such as SciClone (Miller et al., 2014), PyClone (Roth et al., 2014)
85 and MOBSTER (Caravagna et al., 2020a).

86 However, mutation cluster and tumor subclone are not equal items, and mutation
87 co-occurrence is not available in bulk data but needs single-cell resolution
88 confirmation (Gawad et al., 2014; Miles et al., 2020; Wang et al., 2014). Due to the
89 high cost of single-cell DNA sequencing, most of single-cell studies focused on copy
90 number alterations (Bian et al., 2018; Gao et al., 2017; Minussi et al., 2021; Navin et
91 al., 2011), and there are only a few on tumor clonal structures from somatic mutations
92 (Hou et al., 2012; Leung et al., 2017; McPherson et al., 2016). A systematic
93 assessment of the difference of clonal structures from bulk and single-cell resolution

94 analyses for the same tumor is essential to understand to what extent bulk data could
95 depict genuine tumor subclones, but such a study is still lacking.

96 Here, we performed such a study by using both single-cell and bulk mutational
97 data from liver and colorectal cancers, using both public datasets and newly generated
98 data. We identified co-existing tumor subclones by single-cell mutational analysis,
99 despite the absence of subclonal mutation clusters by bulk analysis. The results
100 suggested that genuine tumor clonal structure may not be reliably revealed by bulk
101 approach and will require single-cell dissection.

102

103 **Results**

104 **Pseudo-bulk mutational analysis implied clonal neutral evolution in liver cancer**

105 Inference of tumor subclones based on distribution of bulk-level VAF values is
106 now widely used, and it is generally believed that the presence of mutation VAF
107 clusters represents tumor subclones (Figure 1A). We have recently reconstructed
108 single-variant resolution clonal evolution in liver cancer via patient-specific
109 single-cell target sequencing (Su et al., 2021). As there were great inter-patient
110 heterogeneities, in our previous work we used pseudo-bulk whole exome sequencing
111 (WES) of single-cell genomic amplification mixture to screen for target mutations in
112 each tumor. To better understand the pseudo-bulk mix WES, in this study we also
113 generated true bulk WES data using the same specimens (HCC8-T, HCC8-PVTT,
114 HCC9-T) for systematic comparisons (Figure 1B). The single-cell mutational profiles
115 provided reliable clonal structure landscapes for cross-validation of bulk-level
116 predictions.

117

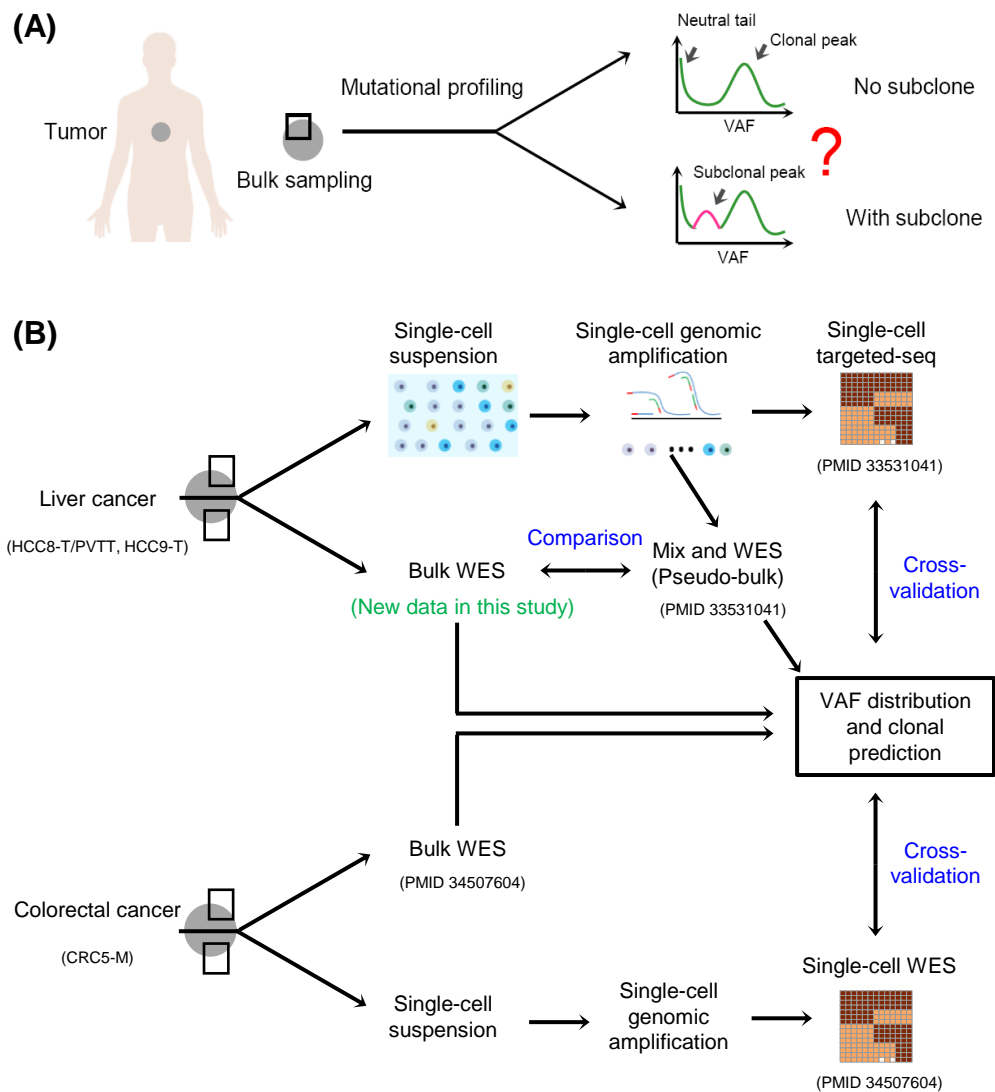


FIGURE 1. Overview of study design. (A) Schematic representation of tumor subclone inference via bulk-level mutational profiling. A typical bulk-level mutation variant allele frequency (VAF) distribution pattern includes a clonal peak and a neutral tail, and a subclonal peak between them is used as an indicator of the presence of a tumor subclone, which may be problematic. (B) Study design. Both liver and colorectal cancer bulk-level and single-cell mutational data were used for clonal structure analysis and cross-validation. For liver cancer, three samples were used (HCC8-T, HCC8-PVTT, HCC9-T), where HCC8-T and HCC8-PVTT are paired primary tumor and metastatic tumor thrombus from the same patient. Single-cell genomic amplification mixtures in liver cancer were used as pseudo-bulk samples for whole exome sequencing (WES), and single-cell targeted sequencing were used to get tumor clonal structures (Data from Su *et al.*, *J Hematol Oncol* 2021, **14**(1):22, PMID 33531041). In this study we also generated new WES data using genuine bulk samples from the same liver cancer samples. For colorectal cancer sample CRC5-M, bulk WES data and single-cell WES data were used for mutation co-occurrence and VAF distribution analysis (Data from Tang *et al.*, *Genome Med* 2021, **13**(1):148, PMID 34507604). Please note in both tumor types, different regions from the same tumor tissue were used separately for single-cell and bulk mutational profiling.

118 For the three liver cancer specimens, the distributions of VAF values from the
119 mix approach exhibited similar pattern, with a clonal peak at VAF ~0.5 and a cell
120 division-related neutral tail containing mainly random mutations at VAF ~0 (Figure
121 2A). It should be noted that the so-called neutral tail may contain low-frequency
122 mutations that are related to future progression. Due to sequencing bias and allelic
123 imbalance in bulk analysis, clonal mutations may span a wide VAF range, and the
124 region between clonal peak and neutral tail is sometimes too narrow to discriminate
125 subclonal VAF clusters. For liver cancer, there were no visible subclonal clusters
126 between clonal peaks and neutral tails using two commonly used clonal analysis tools,
127 SciClone and MOBSTER (Figure 2B,C), suggesting absence of tumor subclones and
128 possibly neutral evolution in all samples (Caravagna et al., 2020a; Williams et al.,
129 2016; Williams et al., 2018).

130

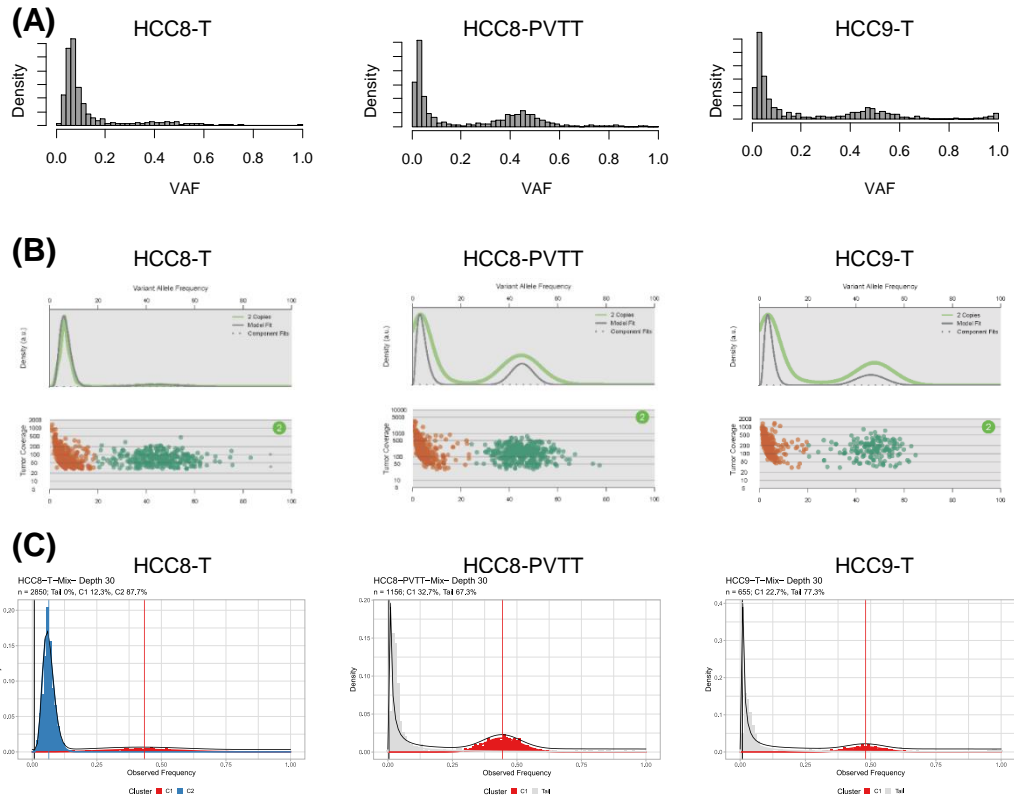


FIGURE 2. Pseudo-bulk mutational analysis implied absence of tumor subclones in liver cancer. (A) Distribution pattern of VAF values for mutations in three liver cancer samples derived from single-cell mix (pseudo-bulk) WES. (B-C) Subclonal deconvolution via SciClone (B) and MOBSTER (C) for the three liver cancer samples. Please note while SciClone assigned the lower range VAF peak in each sample as a tumor subclone, MOBSTER recognized it as neutral tail in HCC8-PVTT and HCC9-T. The C2 cluster in MOBSTER result of HCC8-T should also be neutral tail.

131 **Single-cell analysis revealed co-existing tumor subclones in liver cancer**

132 Single-cell target sequencing of somatic mutations, however, revealed a different
133 scenario of clonal architectures in liver cancer. Co-existing subclones were identified
134 by single-cell analysis in all samples, despite absence of subclonal clusters by bulk
135 analysis. Three co-existing subclones with comparable sizes were identified in
136 HCC8-T (Figure 3A), and the VAF ranges for clonal mutations and different groups of
137 subclonal mutations had overlaps, suggesting that it may be difficult to assign a
138 mutation to a specific subclone based on its bulk VAF value (Figure 3B). Similar
139 results were found in HCC8-PVTT and HCC9-T, with overlaps between different
140 groups of co-mutations, implying that this is a general phenomenon in tumor clonal
141 analysis.

142 Single-cell analysis also provided mutated cell fraction (MCF) value for each
143 mutation, which is actually an indicator of subclone size. There were no overlaps
144 between MCF ranges of clonal and subclonal mutations, although sometimes there
145 were overlaps between MCF values from subclones with similar size (Figure 3B). A
146 comparison of VAF and MCF showed that VAF generally had wider ranges in mix
147 approach which may be more vulnerable to sequencing bias, making it difficult to
148 infer clear clonal structures.

149

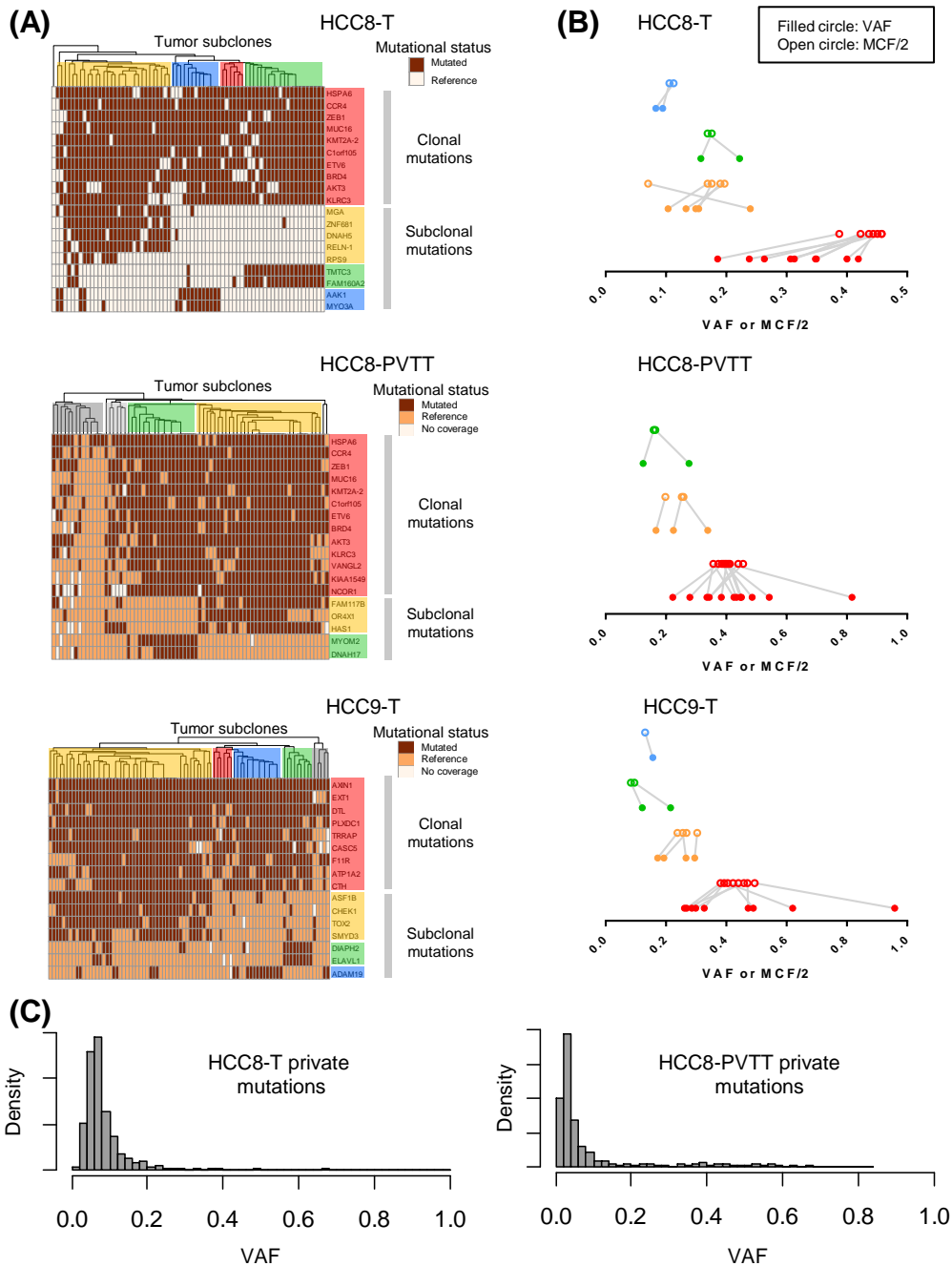


FIGURE 3. Single-cell analysis revealed co-existing tumor subclones in liver cancer not evident in mix approach. (A) Mutation co-occurrence in liver cancer samples revealed by single-cell analysis. Each row represented a somatic mutation and each column represented a cell. The color shading highlighted tumor subclones and corresponding mutations in each group. (B) Comparison of VAF and mutated cell fraction (MCF) values. To adjust for copy numbers, MCF/2 was used for comparison with VAF. Co-mutated clonal and subclonal mutations were grouped by single-cell analysis, with colors consistent with subclonal shading in (A). The lines indicated pairing VAF and MCF/2 for the same mutation. (C) VAF distribution of mutations privately found in HCC8-T or HCC8-PVTT.

150 We then compared the mutations shared by or privately found in one specimens
151 of HCC8-T and HCC8-PVTT, which were paired primary tumor and metastatic tumor
152 thrombus from the same patient. Their shared mutations had higher VAF values, while
153 their private mutations had relatively lower VAF values (Figure S1A). While shared
154 mutations exhibited a clonal peak in both samples (Figure S1B), private mutations in
155 each sample exhibited a neutral tail without detectable subclonal mutation cluster
156 (Figure 3C). The results were consistent with previous finding of common origin and
157 independent evolution for the two tumor specimens (Su et al., 2021). However, the
158 absence of private subclonal clusters were contradicted by the presence of 3 and 2
159 subclones within each sample by single-cell analysis. As the subclonal mutations in
160 primary and metastatic tumors were not shared, they should not be introduced by
161 early stage genetic drift but rather be acquired after occurrence of metastasis (Lynch
162 et al., 2016). The results further supported that absence of subclonal VAF cluster in
163 bulk analysis does not necessarily mean a lack of tumor subclone.

164

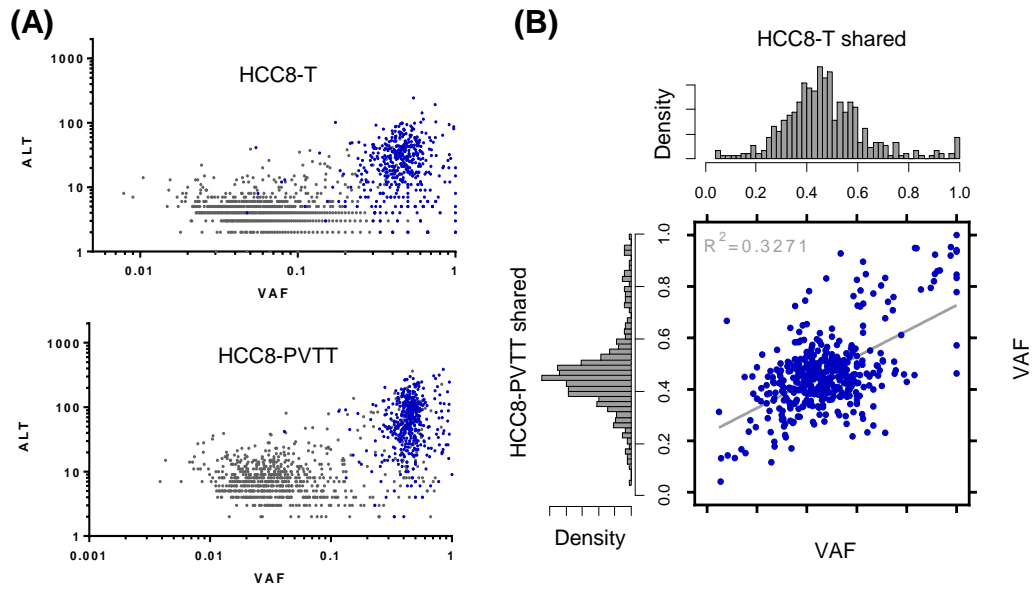


FIGURE S1 VAF distribution patterns of mutations from paired liver cancer samples. (A) Mutation overlaps between paired HCC8-T and HCC8-PVTT. ALT represented numbers of altered reads. Blue dots represented shared mutations, and grey dots represented sample-private mutations. (B) Correlation between VAF values in HCC8-T and HCC8-PVTT for shared mutations, with distribution histogram shown on the top and left for each sample.

165 **No accurate tumor clonal structures in bulk-level analysis**

166 As above tumor clonal analyses were conducted on pseudo-bulk single-cell
167 mixtures, to rule out possible amplification bias or mixing imbalance, we then
168 conducted genuine bulk WES on the same liver cancer samples. Most of mutations
169 detected in the bulk approach were already found in the mix approach, and the latter
170 also had more private mutations (Figure 4A). Different mutations in the two
171 approaches could be attributed to tumor spatial heterogeneity, as they were actually
172 profiling different regions of the same tumor sample (Sun et al., 2017). The shared
173 mutations between two approaches also had higher VAF values while
174 approach-private mutations had relatively lower VAF values (Figure S2A).
175 Correlation analysis of shared mutations showed that VAF values from the bulk
176 approach may be distorted by low tumor purity (Figure S2B).

177 For mutations included in single-cell target sequencing, there were subclonal
178 mutation loss in all bulk samples, causing more simplified tumor clonal structures
179 (Figure 4B). As for the recovered clonal and subclonal mutations, their VAF ranges
180 also had overlaps, just as in the mix approach (Figure 4C). Considering tumor spatial
181 heterogeneity, the results indicated that if bulk sample WES was used to guide
182 downstream single-cell targeted mutational profiling, some subclones may be lost and
183 the heterogeneities will be under-estimated. Besides single-cell mixture WES used in
184 this study, WES using the same cell suspension for single-cell analysis (from the same
185 tumor region) could be another reasonable choice which can be more relevant than
186 neighboring tumor regions.

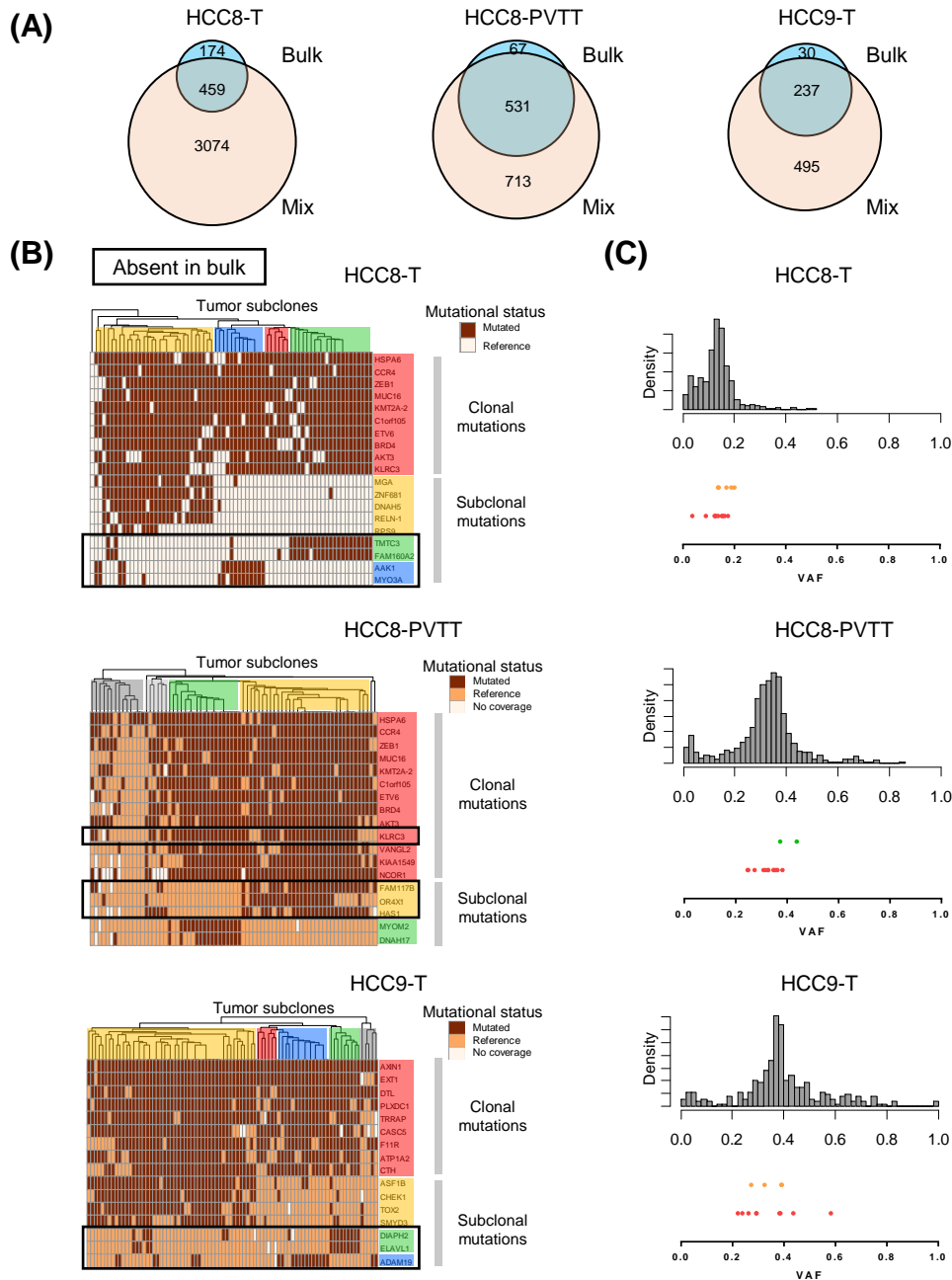


FIGURE 4. Accurate tumor clonal structures could not be revealed by bulk analysis. (A) Mutation overlaps between paired bulk and mix sequencing approaches in three liver cancer samples. (B) Mutations absent in bulk approach analysis shown in black boxes. (C) VAF distribution pattern of co-mutations in the bulk approach. The upper histogram showed VAF distribution of mutations from bulk-level WES, and lower part showed bulk VAF values for clonal and subclonal mutations grouped by single-cell analysis. Each dot represented a mutation, with colors consistent with subclonal shading.

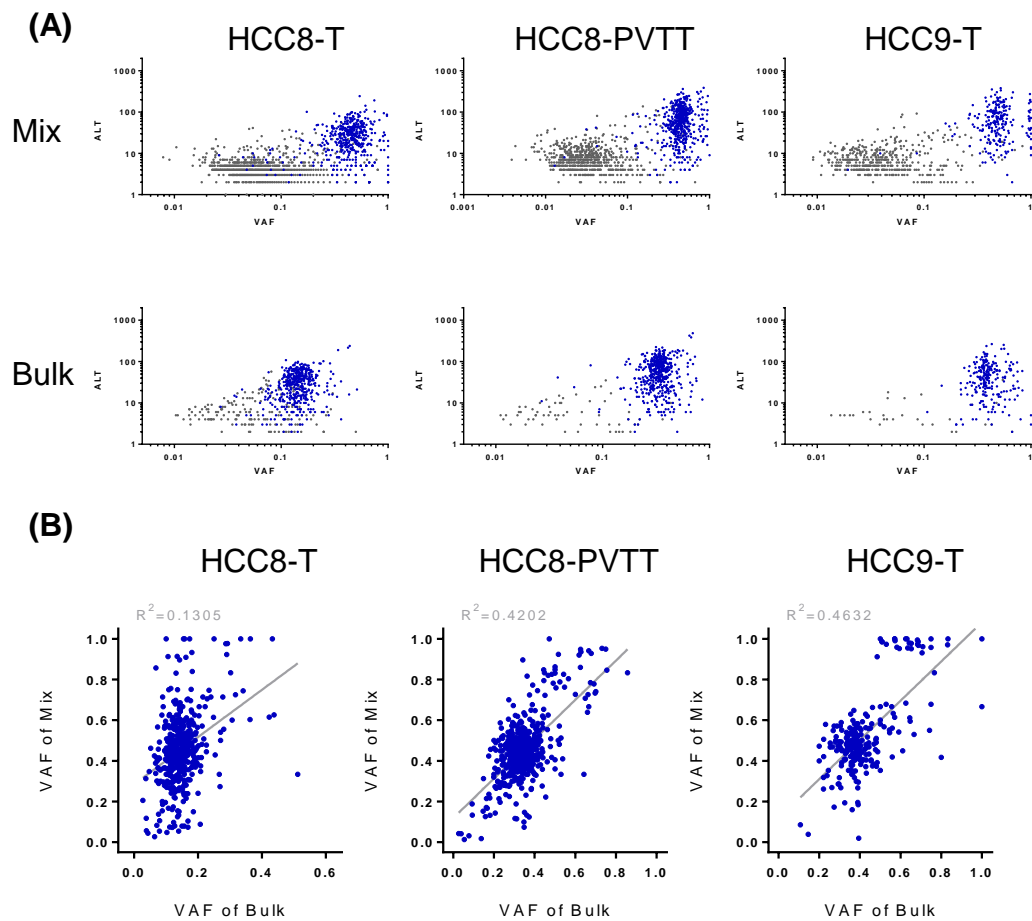


FIGURE S2 Mutation overlaps between bulk and mix sequencing approaches. (A) Mutation overlaps in ALT vs. VAF plot. Blue dots represented shared mutations, and grey dots represented private mutations in each approach. (B) Correlation between VAF values of shared mutations in bulk and mix approaches. The low R^2 value in HCC8-T was caused by low tumor purity in bulk sample.

187 **Different groups of co-mutations could not be discriminated at bulk-level**

188 We then checked whether different groups of co-mutations in liver cancer could
189 be discriminated if other parameter was included besides VAF. As SciClone utilized
190 depth *vs.* VAF for clonal analysis, we considered using ALT (number of altered reads).
191 In the ALT *vs.* VAF plot, mutations in each sample formed two major clusters, with
192 top right cluster representing mainly clonal mutations with higher VAF values and
193 bottom left cluster representing neutral tail mutations with lower VAF values (Figure
194 5A). The region between the two clusters might contain subclonal mutations which
195 may also overlap with the two clusters. As can be seen, co-mutations from single-cell
196 analysis were intermingled together in the mix approach, making it difficult to
197 separate them (Figure 5B). As there were no visible subclonal mutation clusters while
198 single-cell analysis confirmed co-existing subclones, we concluded that accurate
199 tumor clonal structures will require single-cell resolution dissection.

200 In the ALT *vs.* VAF plot for the bulk approach, it was clear that there were less
201 neutral tail mutations compared with the mix approach (Figure 5B and S3), likely due
202 to easier detection of rare mutations in a mixture from less than 100 single cells in
203 comparison with random profiling more than millions of cells in the bulk approach
204 (Figure 5C). Here the clonal and subclonal mutations were also intermingled,
205 supporting that clear discrimination of co-mutations might be challenging in bulk
206 approach, no matter from pseudo-bulk or genuine bulk samples.

207

208

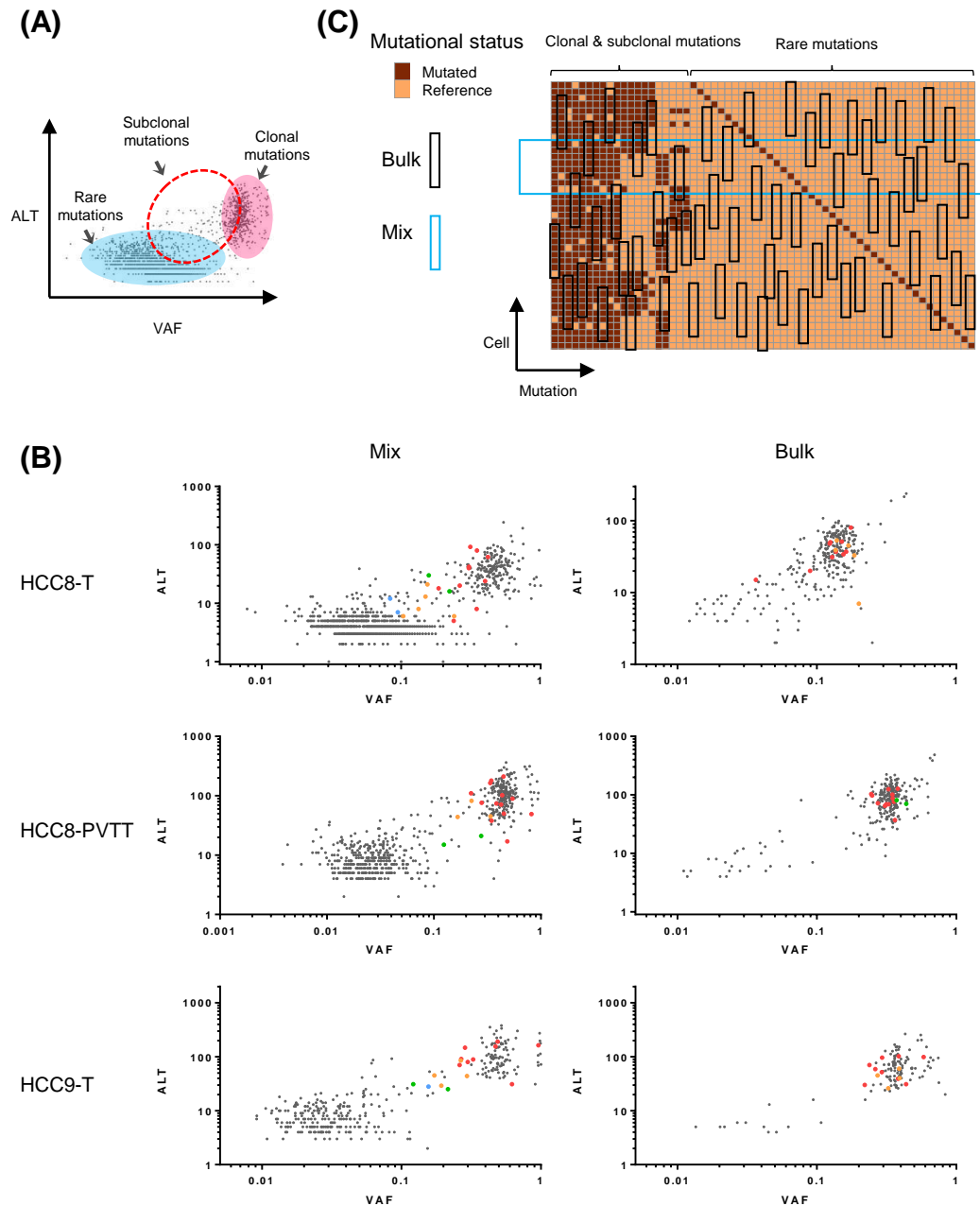


FIGURE 5. Different groups of co-mutations could not be discriminated in ALT vs. VAF plot. (A) Schematic representation of clonal, subclonal and rare mutations in ALT vs. VAF plot. (B) Distribution patterns of co-mutations in ALT vs. VAF plot in mix and bulk approaches. Color dots represented co-mutations from single-cell analysis, and grey dots represented other exonic mutations. (C) Sampling strategy difference between bulk and mix sequencing approaches. For single-cell mix approach, most clonal, subclonal and rare mutations are recovered as the sequencing coverage is at similar level with the number of single cells mixed (represented by the big blue box). For bulk approach, rare mutations will be easily lost due to random sampling at each mutation site (represented by the black box at each site).

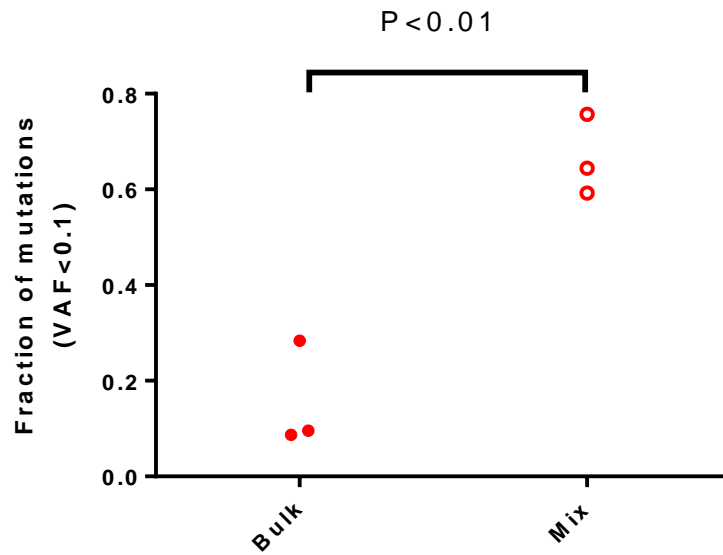


FIGURE S3 Comparison of neutral tail size in the bulk and mix sequencing approaches. The fraction of exonic mutations with VAF<0.1 was used as indicator of the neutral tail size for HCC8-T, HCC8-PVTT and HCC9-T. Paired *t* test (Two-tailed) was performed to check the statistical significance between the bulk and mix approaches.

209 **Dynamic evolution hidden under clonal neutral appearance at bulk-level**

210 Single-cell WES has genomic coverage advantage in comparison with targeted
211 sequencing, which will make clonal structure more reliable. As single-cell analyses in
212 liver cancer were based on targeted sequencing, to rule out possible target selection
213 bias or amplification distortion, we then analyzed a single-cell exonic mutational
214 dataset from colorectal cancer (Tang et al., 2021). Sample CRC5-M exhibited
215 branched evolution with step-by-step subclonal mutation acquisition and further split
216 of each subclone (Figure 6A), demonstrating the complex relationship between
217 subclonal mutation clusters and tumor subclones as the possession of a group of
218 subclonal mutations may not always define a homogenous tumor subclone.

219

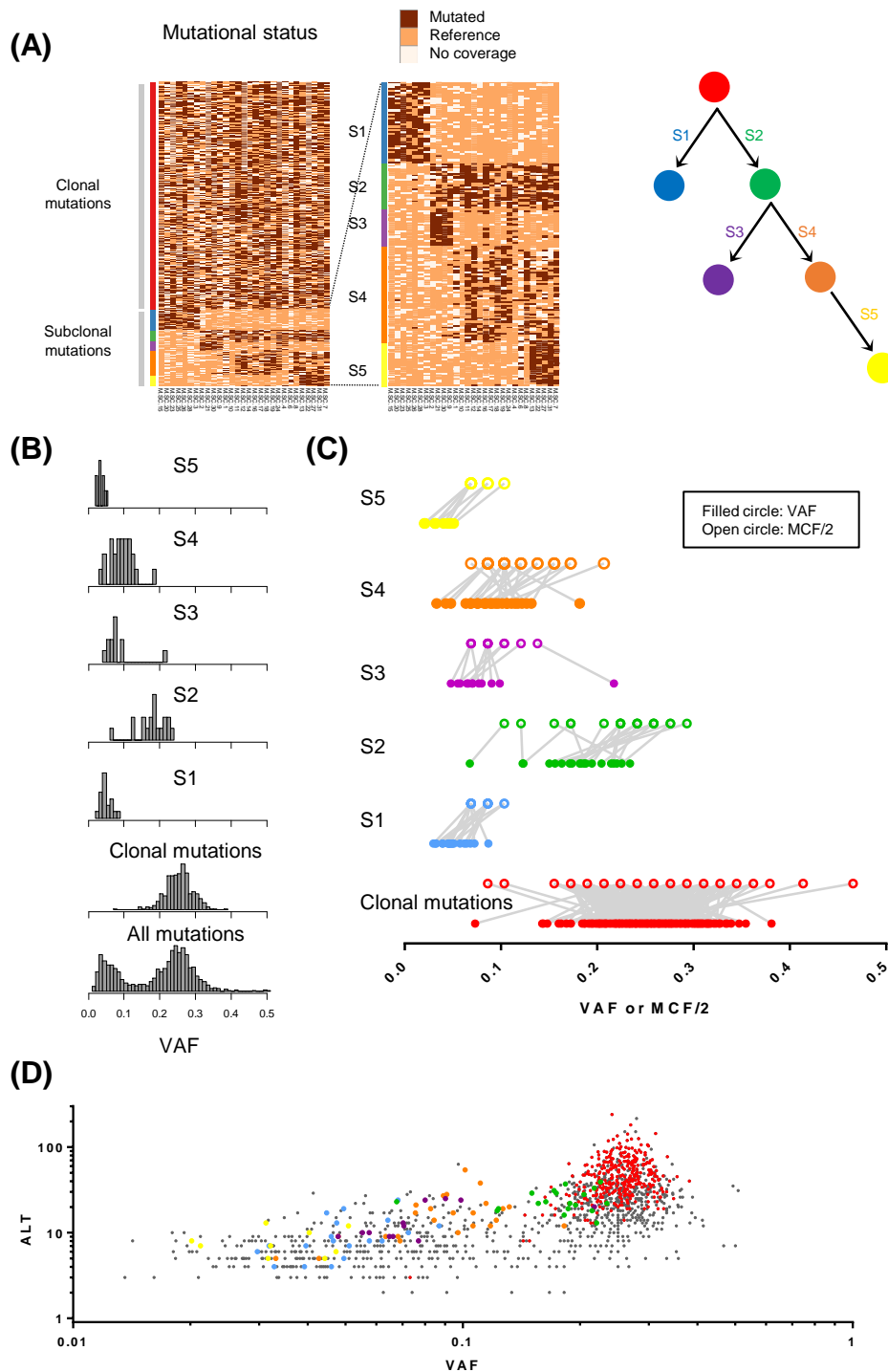


FIGURE 6. Dynamic evolution hidden under clonal neutral appearance at bulk-level in colorectal cancer. (A) Mutation co-occurrence in colorectal cancer sample CRC5-M revealed by single-cell WES. S1-S5 were subclonal mutation groups, and their acquisition order was shown on the right. (B) VAF distribution pattern of co-mutations. The histograms showed VAF distribution of different groups of subclonal mutations (S1-S5), clonal mutations, and all mutations from bulk-level WES. Please note the subclonal peaks were not reflected in the final histogram. (C) Comparison of VAF and MCF/2 values in co-mutated clonal and subclonal mutations, with colors consistent with subclonal shading in (A). The lines indicated pairing VAF and MCF/2 for the same mutation. (D) Distribution patterns of different groups of co-mutations in ALT vs. VAF plot.

220 Using the co-mutation groups defined by single-cell WES, we then checked their
221 bulk VAF ranges in CRC5-M. Despite the complicated subclonal structure revealed
222 by single-cell analysis, the VAF distribution showed a typical clonal peak and a
223 neutral tail, and different groups of subclonal mutations were not reflected by
224 corresponding subclonal peaks (Figure 6B). The VAF ranges of clonal mutations and
225 Group S2 subclonal mutations had overlaps, while other groups of subclonal
226 mutations (Group S1, S3, S4, S5) also had overlaps (Figure 6C). The ranges of VAF
227 and MCF values for different co-mutation groups showed very good consistency in
228 CRC5-M (Figure 6C), indicating reliable allelic representation in bulk exonic scale
229 mutational profiling. In the ALT *vs.* VAF plot, the results also showed difficulty in
230 discriminating different groups of co-mutations (Figure 6D). The analysis showed that
231 tumor clonal structure was hidden under the seemingly clonal neutral pattern of bulk
232 analysis, and accurate clonal structure and dynamic evolution will thus require
233 investigation at single-cell resolution (Figure 7).

234

235

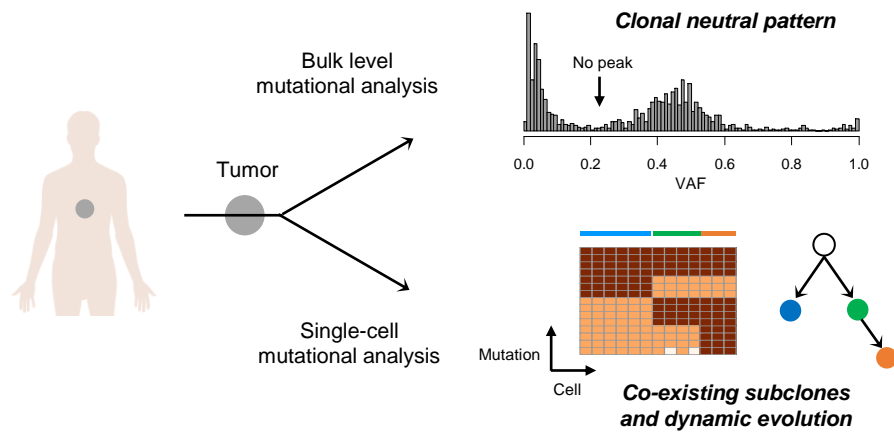


FIGURE 7. Schematic diagram showing the main finding. Complex tumor clonal structure and dynamic evolution could be revealed by single-cell analysis, which may be hidden under clonal neutral pattern in bulk analysis.

236 **Discussion**

237 Bulk-level tumor clonal analysis has improved our understanding of intra-tumor
238 heterogeneity, but it may not be able to reveal accurate tumor clonal architecture or
239 reconstruct evolutionary history (Alves et al., 2017; Lim et al., 2020; Turajlic et al.,
240 2019). Recently, a method that combined machine learning and population genetics
241 was developed to enable more accurate subclonal reconstruction by ruling out
242 interference from cell-division related neutral tail (Caravagna et al., 2020a). Ongoing
243 subclonal selection was detected in 9 out of 298 high quality diploid tumor cases from
244 PCAWG data, and prevalent neutral evolutionary pattern was proposed among tumors
245 (Caravagna et al., 2020a). Here our analyses suggested that for some cases, the
246 absence of subclonal mutation clusters does not necessarily support clonal neutral
247 evolution, and utilization of such a criteria may underestimate the prevalence of tumor
248 subclonal heterogeneity. Interpretation of clonal heterogeneity in bulk tumor samples
249 should thus be careful, and systematic re-assessment of genetic heterogeneity in major
250 tumor atlas datasets would be beneficial.

251 A major limit of bulk approach clonal analysis is the gap between mutation VAF
252 cluster and tumor subclone, as they are two different terms that may not be exactly
253 matched. For example, depending on the emerging stages of subclones during tumor
254 progression, their subclone-specific mutations may not necessarily form apparent and
255 detectable VAF clusters, especially for early subclones containing less mutations
256 (Williams et al., 2018). Moreover, if there are subclones co-existing within a tumor at
257 similar prevalence, their mutation VAF ranges will inevitably overlap and be difficult

258 to separate. Tumor purity and genomic copy number status will further complicate the
259 condition (Salcedo et al., 2020; Tarabichi et al., 2021), and clonal structure revelation
260 thus calls for single-cell analysis (Davis et al., 2017; Evrony et al., 2021).

261 As it is difficult to obtain longitudinal specimens, dissection of clonal evolution is
262 particularly challenging for solid tumors (Bailey et al., 2021). Single-cell profiling of
263 tumor tissues based on somatic mutations will facilitate clonal history reconstruction
264 at unprecedented accuracy, even for samples collected at a single time point (Dong et
265 al., 2017; Evrony et al., 2021; Su et al., 2021). On account of still expensive whole
266 genomic or exonic scale mutational analyses, however, the number of single cells
267 profiled is still limited to hundreds for single-variant resolution studies (Duan et al.,
268 2018; Tang et al., 2021; Wang et al., 2014). This will cause cell selection bias and lose
269 rare subclones which might hold keys for treatment resistance or metastasis.
270 Moreover, the spatial heterogeneity also makes it necessary to profile more than one
271 region in a tumor by single-cell analysis, and this will need analysis of even more
272 single cells. Current numbers of single cells analyzed were still a biased sampling of
273 the tremendous genetic heterogeneities within tumors, and we expect future
274 technological advances that enable mutational profiling of more single cells to shed
275 light on tumor evolution and therapy design.

276 In summary, here we demonstrated that bulk-level analyses may be ill-suited for
277 revealing tumor clonal structure due to difference between mutation cluster and tumor
278 subclone. The absence of subclonal mutation cluster does not necessarily support

279 clonal neutral evolution, and tumor clonal structure and evolution history can be
280 better unveiled by single-cell analysis.

281

282 **Methods**

283 **Clinical specimens and sequencing strategies of liver cancer**

284 Single-cell mix (pseudo-bulk) WES and single-cell target mutation data from 3
285 liver cancer specimens were used in this study: HCC8-T, HCC8-PVTT and HCC9-T,
286 in which HCC8-T and HCC8-PVTT were paired primary tumor and metastatic tumor
287 thrombus from the same patient. Other samples with allelic dropout (ADO) issue or
288 without subclones were not included in this study. Whole genome amplification
289 product of single cells derived from paratumor and tumor tissues were separately
290 mixed for WES, and ~60 putative clonal and subclonal mutation sites were then
291 selected from each patient for single-cell target sequencing (Su et al., 2021). The
292 sequencing data for mix approach WES of HCC8-T, HCC8-PVTT and HCC9-T were
293 obtained from project PRJNA606993 in NCBI SRA database, with BioSample
294 accession number SAMN14118840, SAMN14118841 and SAMN14118843.

295 As a comparison between pseudo-bulk and genuine bulk approaches, the 3 liver
296 cancer specimens also underwent bulk-level WES using Agilent SureSelect Human
297 All Exon v7 Kit (Agilent, 5191-4005) and illumina NovaSeq 2 × 150 bp sequencing
298 mode. Sequencing reads were mapped to GRCh37/hg19 with BWA (Li and Durbin,
299 2009), mutations were called with GATK Mutect2 (McKenna et al., 2010), and SNPs
300 were filtered using dbSNP141 (Sherry et al., 2001) and 1,000 Genomes Project (v3)

301 database (Auton et al., 2015). The median sequencing depths for the tumor samples
302 were more than 100×. The study was approved by the Ethnical Review Board of
303 Shanghai Jiao Tong University, and the protocol conformed to the ethical guidelines
304 of the 1975 Declaration of Helsinki.

305

306 **Subclonal deconvolution in liver cancer by mix approach sequencing**

307 After calling mutations from each tumor sample, VAF values were calculated for
308 all mutations. Two tumor clonal analysis tools, SciClone (Miller et al., 2014) and
309 MOBSTER (Caravagna et al., 2020a; Caravagna et al., 2020b), were then used to
310 infer subclones in liver cancer samples. While SciClone separated the clonal peak
311 (VAF ~0.5) and neutral tail (VAF ~0) but assigned both as subclones, MOBSTER
312 could further recognize neutral tail in some cases.

313

314 **Tumor subclones and co-mutations in liver cancer single-cell data**

315 Single-cell mutational data were used to investigate the clonal structures and
316 mutation co-occurrence in each tumor case. After strict quality control, 71, 74 and 84
317 single cells from HCC8-T, HCC8-PVTT and HCC9-T were used for downstream
318 analysis. Based on the mutational status of somatic mutations, single cells in each
319 tumor were clustered into subclones. Clustering of mutations grouped them into
320 clonal mutations present in all tumor cells, or subclonal co-mutations specifically
321 found in each tumor subclone.

322 MCF for each mutation was calculated as the fraction of single cells harboring
323 that mutation in a given tumor sample. Considering the effect of copy numbers, the
324 ranges of VAF values in the mix approach and their corresponding MCF/2 values
325 were compared to investigate the difference between mutation clusters and tumor
326 subclones.

327

328 **Comparison of mutations in paired primary and metastatic liver tumors**

329 For the paired HCC8-T and HCC8-PVTT, the plot of ALT *vs.* VAF (Shi et al.,
330 2018) was used to check the VAF ranges of the shared and private mutations in each
331 sample. The VAF distribution patterns of mutations shared by them or privately found
332 in only one sample were compared to find possible subclonal peaks.

333

334 **Comparison of mutations in liver cancer by mix and bulk approaches**

335 The numbers of shared and approach-private mutations were analyzed for the
336 bulk and mix approaches. The plot of ALT *vs.* VAF was used to check the VAF ranges
337 of the shared and private mutations in each approach. The correlation of VAF values
338 between the two approaches for shared mutations were analyzed to check the extent
339 of VAF deviation in different approaches, and recovery and loss of single-cell target
340 mutations in the bulk approach were also analyzed to compare clonal structure
341 difference. The VAF distribution patterns of mutations from the two approaches were
342 shown in histogram plot. After clonal and subclonal mutations were grouped by
343 single-cell analysis, VAF values of those grouped mutations in both mix and bulk

344 approaches were compared to check range overlaps and relative locations to
345 mutational peaks. The plot of ALT vs. VAF was also used to check the possibility of
346 discriminating different groups of co-mutations in both bulk and mix approaches. The
347 fractions of exonic mutations with VAF <0.1 were calculated for comparison of
348 neutral tail sizes in the mix and bulk sequencing approaches.

349

350 **Subclonal analysis of colorectal cancer**

351 A recent work reported the clonal structure of both primary colorectal cancer and
352 metastases based on single-cell WES, providing unbiased exonic scale single-cell
353 mutational profiles (Tang et al., 2021). Here sample CRC5-M was chosen for
354 subclonal analysis as it was the sample with the most complicated subclonal structure
355 and available bulk WES data. Mutation co-occurrences were revealed by single-cell
356 analysis, and bulk VAF values of those co-mutations were compared to check range
357 overlaps. A comparison of ranges of VAF and MCF/2 values for different groups of
358 co-mutations were also performed. The plot of ALT vs. VAF was also used to check
359 the possibility of discriminating different groups of co-mutations.

360

361 **Statistical analysis**

362 Correlation analysis between two datasets were performed using GraphPad Prism
363 6, and R square values were provided for each analysis. Paired *t* test (Two-tailed) was
364 performed to check the statistical significance between neutral tail sizes in the bulk
365 and mix sequencing approaches in liver cancer.

366

367 **Data and materials availability**

368 The sequencing data for bulk approach WES have been deposited in NCBI SRA
369 database under project PRJNA606993, with BioSample accession number
370 SAMN21591192, SAMN21591193 and SAMN21591194 for HCC8-T, HCC8-PVTT
371 and HCC9-T. All other relevant data are available upon request.

372

373 **Acknowledgement**

374 We would like to thank Professor Dan Xie and Dr. Kailing Tu from West China
375 Hospital, Sichuan University for help with the single-cell WES data of colorectal
376 cancer. This work was supported in part by National Natural Science Foundation of
377 China (81802806, 31900484, 81902561), Guangdong Province Science and
378 Technology Program (2020A1515010919), Natural Science Foundation of Shanghai
379 (20511101900, 20ZR1427200), Shanghai Pujiang Program (20PJ1409800), SJTU
380 Scientific and Technological Innovation Funds (2019TPA09) and SJTU
381 Interdisciplinary Program (YG2021QN80).

382

383 **Author contributions**

384 **X. Su:** Conception and design, methodology, formal analysis, investigation, data
385 curation, writing - original draft, supervision, project administration. **S. Bai:** Formal
386 analysis, writing - review & editing. **G. Xie:** Formal analysis, writing - review &
387 editing. **Y. Shi:** Formal analysis, writing - review & editing. **L. Zhao:** Methodology,

388 data curation. **G. Yang:** Data curation. **F. Tian:** Writing - review & editing. **K. He:**
389 Investigation. **L. Wang:** Investigation. **Q. Long:** Conception and design, supervision,
390 writing - review & editing. **Z. Han:** Conception and design, supervision, writing -
391 original draft.

392

393 **References**

394 Alves, J.M., Prieto, T., and Posada, D. (2017). Multiregional Tumor Trees Are Not Phylogenies. *Trends*
395 *Cancer* 3, 546-550.

396 Auton, A., Brooks, L.D., Durbin, R.M., Garrison, E.P., Kang, H.M., Korbel, J.O., Marchini, J.L.,
397 McCarthy, S., McVean, G.A., and Abecasis, G.R. (2015). A global reference for human genetic
398 variation. *Nature* 526, 68-74.

399 Bailey, C., Black, J.R.M., Reading, J.L., Litchfield, K., Turajlic, S., McGranahan, N., Jamal-Hanjani,
400 M., and Swanton, C. (2021). Tracking Cancer Evolution through the Disease Course. *Cancer Discov* 11,
401 916-932.

402 Bian, S., Hou, Y., Zhou, X., Li, X., Yong, J., Wang, Y., Wang, W., Yan, J., Hu, B., Guo, H., *et al.* (2018).
403 Single-cell multiomics sequencing and analyses of human colorectal cancer. *Science* 362, 1060-1063.

404 Cairns, J. (1975). Mutation selection and the natural history of cancer. *Nature* 255, 197-200.

405 Caravagna, G., Heide, T., Williams, M.J., Zapata, L., Nichol, D., Chkhaidze, K., Cross, W., Cresswell,
406 G.D., Werner, B., Acar, A., *et al.* (2020a). Subclonal reconstruction of tumors by using machine
407 learning and population genetics. *Nat Genet* 52, 898-907.

408 Caravagna, G., Sanguinetti, G., Graham, T.A., and Sottoriva, A. (2020b). The MOBSTER R package
409 for tumour subclonal deconvolution from bulk DNA whole-genome sequencing data. *BMC*
410 *Bioinformatics* 21, 531.

411 Davis, A., Gao, R., and Navin, N. (2017). Tumor evolution: Linear, branching, neutral or punctuated?
412 *Biochim Biophys Acta Rev Cancer* 1867, 151-161.

413 Dentre, S.C., Leshchiner, I., Haase, K., Tarabichi, M., Wintersinger, J., Deshwar, A.G., Yu, K.,
414 Rubanova, Y., Macintyre, G., Demeulemeester, J., *et al.* (2021). Characterizing genetic intra-tumor
415 heterogeneity across 2,658 human cancer genomes. *Cell* 184, 2239-2254.

416 Dong, X., Zhang, L., Milholland, B., Lee, M., Maslov, A.Y., Wang, T., and Vijg, J. (2017). Accurate
417 identification of single-nucleotide variants in whole-genome-amplified single cells. *Nat Methods* 14,
418 491-493.

- 419 Duan, M., Hao, J.F., Cui, S.J., Worthley, D.L., Zhang, S., Wang, Z.C., Shi, J.Y., Liu, L.Z., Wang, X.Y.,
420 Ke, A.W., *et al.* (2018). Diverse modes of clonal evolution in HBV-related hepatocellular carcinoma
421 revealed by single-cell genome sequencing. *Cell Res* 28, 359-373.
- 422 Evrony, G.D., Hinch, A.G., and Luo, C. (2021). Applications of Single-Cell DNA Sequencing. *Annu*
423 *Rev Genomics Hum Genet* 22, 171-197.
- 424 Gao, Y., Ni, X., Guo, H., Su, Z., Ba, Y., Tong, Z., Guo, Z., Yao, X., Chen, X., Yin, J., *et al.* (2017).
425 Single-cell sequencing deciphers a convergent evolution of copy number alterations from primary to
426 circulating tumor cells. *Genome Res* 27, 1312-1322.
- 427 Gawad, C., Koh, W., and Quake, S.R. (2014). Dissecting the clonal origins of childhood acute
428 lymphoblastic leukemia by single-cell genomics. *Proc Natl Acad Sci U S A* 111, 17947-17952.
- 429 Gerstung, M., Jolly, C., Leshchiner, I., Dentre, S.C., Gonzalez, S., Rosebrock, D., Mitchell, T.J.,
430 Rubanova, Y., Anur, P., Yu, K., *et al.* (2020). The evolutionary history of 2,658 cancers. *Nature* 578,
431 122-128.
- 432 Greaves, M., and Maley, C.C. (2012). Clonal evolution in cancer. *Nature* 481, 306-313.
- 433 Hou, Y., Song, L.T., Zhu, P., Zhang, B., Tao, Y., Xu, X., Li, F.Q., Wu, K., Liang, J., Shao, D., *et al.*
434 (2012). Single-Cell Exome Sequencing and Monoclonal Evolution of a JAK2-Negative
435 Myeloproliferative Neoplasm. *Cell* 148, 873-885.
- 436 Jamal-Hanjani, M., Wilson, G.A., McGranahan, N., Birkbak, N.J., Watkins, T.B.K., Veeriah, S., Shafi,
437 S., Johnson, D.H., Mitter, R., Rosenthal, R., *et al.* (2017). Tracking the Evolution of Non-Small-Cell
438 Lung Cancer. *N Engl J Med* 376, 2109-2121.
- 439 Leung, M.L., Davis, A., Gao, R., Casasent, A., Wang, Y., Sei, E., Vilar, E., Maru, D., Kopetz, S., and
440 Navin, N.E. (2017). Single-cell DNA sequencing reveals a late-dissemination model in metastatic
441 colorectal cancer. *Genome Res* 27, 1287-1299.
- 442 Li, H., and Durbin, R. (2009). Fast and accurate short read alignment with Burrows-Wheeler transform.
443 *Bioinformatics* 25, 1754-1760.
- 444 Lim, B., Lin, Y., and Navin, N. (2020). Advancing Cancer Research and Medicine with Single-Cell
445 Genomics. *Cancer Cell* 37, 456-470.
- 446 Lynch, M., Ackerman, M.S., Gout, J.F., Long, H., Sung, W., Thomas, W.K., and Foster, P.L. (2016).
447 Genetic drift, selection and the evolution of the mutation rate. *Nat Rev Genet* 17, 704-714.
- 448 Marusyk, A., Janiszewska, M., and Polyak, K. (2020). Intratumor Heterogeneity: The Rosetta Stone of
449 Therapy Resistance. *Cancer Cell* 37, 471-484.
- 450 McKenna, A., Hanna, M., Banks, E., Sivachenko, A., Cibulskis, K., Kernytsky, A., Garimella, K.,
451 Altschuler, D., Gabriel, S., Daly, M., *et al.* (2010). The Genome Analysis Toolkit: a MapReduce
452 framework for analyzing next-generation DNA sequencing data. *Genome Res* 20, 1297-1303.

- 453 McPherson, A., Roth, A., Laks, E., Masud, T., Bashashati, A., Zhang, A.W., Ha, G., Biele, J., Yap, D.,
454 Wan, A., *et al.* (2016). Divergent modes of clonal spread and intraperitoneal mixing in high-grade
455 serous ovarian cancer. *Nat Genet* *48*, 758-767.
- 456 Miles, L.A., Bowman, R.L., Merlinsky, T.R., Csete, I.S., Ooi, A.T., Durruthy-Durruthy, R., Bowman,
457 M., Famulare, C., Patel, M.A., Mendez, P., *et al.* (2020). Single-cell mutation analysis of clonal
458 evolution in myeloid malignancies. *Nature* *587*, 477-482.
- 459 Miller, C.A., White, B.S., Dees, N.D., Griffith, M., Welch, J.S., Griffith, O.L., Vij, R., Tomasson, M.H.,
460 Graubert, T.A., Walter, M.J., *et al.* (2014). SciClone: inferring clonal architecture and tracking the
461 spatial and temporal patterns of tumor evolution. *PLoS Comput Biol* *10*, e1003665.
- 462 Minussi, D.C., Nicholson, M.D., Ye, H., Davis, A., Wang, K., Baker, T., Tarabichi, M., Sei, E., Du, H.,
463 Rabbani, M., *et al.* (2021). Breast tumours maintain a reservoir of subclonal diversity during expansion.
464 *Nature* *592*, 302-308.
- 465 Navin, N., Kendall, J., Troge, J., Andrews, P., Rodgers, L., McIndoo, J., Cook, K., Stepansky, A., Levy,
466 D., Esposito, D., *et al.* (2011). Tumour evolution inferred by single-cell sequencing. *Nature* *472*, 90-94.
- 467 Nowell, P.C. (1976). The clonal evolution of tumor cell populations. *Science* *194*, 23-28.
- 468 Roth, A., Khattra, J., Yap, D., Wan, A., Laks, E., Biele, J., Ha, G., Aparicio, S., Bouchard-Cote, A., and
469 Shah, S.P. (2014). PyClone: statistical inference of clonal population structure in cancer. *Nat Methods*
470 *11*, 396-398.
- 471 Salcedo, A., Tarabichi, M., Espiritu, S.M.G., Deshwar, A.G., David, M., Wilson, N.M., Dentre, S.,
472 Wintersinger, J.A., Liu, L.Y., Ko, M., *et al.* (2020). A community effort to create standards for
473 evaluating tumor subclonal reconstruction. *Nat Biotechnol* *38*, 97-107.
- 474 Sherry, S.T., Ward, M.H., Kholodov, M., Baker, J., Phan, L., Smigielski, E.M., and Sirotkin, K. (2001).
475 dbSNP: the NCBI database of genetic variation. *Nucleic Acids Res* *29*, 308-311.
- 476 Shi, W., Ng, C.K.Y., Lim, R.S., Jiang, T., Kumar, S., Li, X., Wali, V.B., Piscuoglio, S., Gerstein, M.B.,
477 Chagpar, A.B., *et al.* (2018). Reliability of Whole-Exome Sequencing for Assessing Intratumor Genetic
478 Heterogeneity. *Cell Rep* *25*, 1446-1457.
- 479 Su, X.B., Zhao, L.N., Shi, Y., Zhang, R., Long, Q., Bai, S.H., Luo, Q., Lin, Y.X., Zou, X., Ghazanfar, S.,
480 *et al.* (2021). Clonal evolution in liver cancer at single-cell and single-variant resolution. *J Hematol*
481 *Oncol* *14*, 22.
- 482 Sun, R., Hu, Z., Sottoriva, A., Graham, T.A., Harpak, A., Ma, Z., Fischer, J.M., Shibata, D., and Curtis,
483 C. (2017). Between-region genetic divergence reflects the mode and tempo of tumor evolution. *Nat*
484 *Genet* *49*, 1015-1024.
- 485 Tang, J., Tu, K., Lu, K., Zhang, J., Luo, K., Jin, H., Wang, L., Yang, L., Xiao, W., Zhang, Q., *et al.*
486 (2021). Single-cell exome sequencing reveals multiple subclones in metastatic colorectal carcinoma.
487 *Genome Med* *13*, 148.

- 488 Tarabichi, M., Salcedo, A., Deshwar, A.G., Ni Leathlobhair, M., Wintersinger, J., Wedge, D.C., Van
489 Loo, P., Morris, Q.D., and Boutros, P.C. (2021). A practical guide to cancer subclonal reconstruction
490 from DNA sequencing. *Nat Methods* *18*, 144-155.
- 491 Turajlic, S., Sottoriva, A., Graham, T., and Swanton, C. (2019). Resolving genetic heterogeneity in
492 cancer. *Nat Rev Genet* *20*, 404-416.
- 493 Turajlic, S., Xu, H., Litchfield, K., Rowan, A., Chambers, T., Lopez, J.I., Nicol, D., O'Brien, T., Larkin,
494 J., Horswell, S., *et al.* (2018). Tracking Cancer Evolution Reveals Constrained Routes to Metastases:
495 TRACERx Renal. *Cell* *173*, 581-594.
- 496 Wang, Y., Waters, J., Leung, M.L., Unruh, A., Roh, W., Shi, X., Chen, K., Scheet, P., Vattathil, S., Liang,
497 H., *et al.* (2014). Clonal evolution in breast cancer revealed by single nucleus genome sequencing.
498 *Nature* *512*, 155-160.
- 499 Williams, M.J., Werner, B., Barnes, C.P., Graham, T.A., and Sottoriva, A. (2016). Identification of
500 neutral tumor evolution across cancer types. *Nat Genet* *48*, 238-244.
- 501 Williams, M.J., Werner, B., Heide, T., Curtis, C., Barnes, C.P., Sottoriva, A., and Graham, T.A. (2018).
502 Quantification of subclonal selection in cancer from bulk sequencing data. *Nat Genet* *50*, 895-903.
- 503 Yates, L.R., and Campbell, P.J. (2012). Evolution of the cancer genome. *Nat Rev Genet* *13*, 795-806.
- 504 Zahir, N., Sun, R., Gallahan, D., Gatenby, R.A., and Curtis, C. (2020). Characterizing the ecological
505 and evolutionary dynamics of cancer. *Nat Genet* *52*, 759-767.
- 506
- 507